

Structure-Property Relationship in Heat-Set Poly(ethylene Terephthalate) Fibers. II. Thermal Behavior and Morphology

V. B. GUPTA, C. RAMESH, and A. K. GUPTA, *Department of Textile Technology and Center for Materials Science and Technology, Indian Institute of Technology, Delhi, New Delhi-110016, India*

Synopsis

Thermal behavior of drawn poly(ethylene terephthalate) (PET) multifilament yarn which had earlier been heat-set at various temperatures between 100°C and 250°C under "free to relax" and "taut at constant length" conditions is studied by differential scanning calorimetric (DSC) measurements. Structural studies are made by X-ray diffraction and infrared absorption spectrophotometry. Two interesting observations are reported: (i) In the taut-annealed samples, the noncrystallizable fraction increases and crystallizable fraction decreases with increasing heat-setting temperature; the free-annealed samples show the opposite effect; and (ii) a well-crystallized free-annealed sample melts at a higher temperature than the corresponding taut-annealed sample. Both these observations are interpreted in terms of sample morphology; the free-annealed samples have more perfect crystals and a more distinct separation between the crystalline and amorphous phases which facilitates transport and diffusion resulting in an ease of reorganization.

INTRODUCTION

There has been considerable interest in trying to understand the dependence of the melting behavior of poly(ethylene terephthalate) (PET) in the semicrystalline state with different thermal histories on its morphology.¹⁻⁹ PET crystallized under isothermal conditions often shows double melting endotherms, which have been attributed to partial melting of crystallites formed at the crystallization temperature followed by rapid crystallization during scanning in differential scanning calorimetry (DSC) experiment. The literature on thermal analysis of PET up to 1980 has been summarized in Ref. 10. In a series of papers on isothermally crystallized semicrystalline isotropic PET, Groeninckx and co-workers⁷⁻⁹ have concluded that, in samples showing double-peak endotherms, the higher melting temperature species represents the less stable fraction, which undergoes reorganization. This reorganization involves only crystal perfection and/or crystal thickening. They also postulate that in high temperature annealing crystal perfection occurs at the boundary layers of the crystalline and amorphous phases.

The morphological features which influence the melting behavior of drawn PET fibers have not been clearly identified. When commercial PET multifilament yarn is heat-set under free-to-relax or under taut-at-constant length conditions, important structural and morphological differences between the two sets of samples have been observed.¹¹⁻¹³ These differences

result in considerable differences in the mechanical behaviors of these samples.¹³⁻¹⁵ The major structural difference is that the free-annealed samples have much lower amorphous orientation, while the major morphological difference is the relatively more distinct phase separation of the crystalline and amorphous regions in these samples with a predominantly series type coupling between the two phases. It was therefore considered worthwhile studying their thermal behaviors. Possible morphological origins for the thermal effects are discussed.

EXPERIMENTAL

Sample Preparation. The starting material was a drawn (draw ratio 3.92) commercial multifilament yarn 76/36/0, i.e., 76 denier, 36 filament, and zero twist. The sample will be referred to as the "control" and has been described in detail elsewhere.¹¹ The yarn was heat-set in a silicone oil bath maintained at a fixed temperature within $\pm 2^\circ\text{C}$. The heat-setting was done at 100°C, 120°C, 140°C, 160°C, 180°C, 200°C, 220°C, 230°C, 240°C, and 250°C under two conditions, viz., when the yarn was (i) held at constant length (designated TA or taut-annealed) and (ii) free to relax (FA or free-annealed), at each temperature for 5 min. The 240°C and 250°C heat-set samples were also prepared with heat-setting times of 30 min and 60 min. The samples were taken out of the bath and allowed to reach ambient temperature; they were blotted, then given a wash in carbon tetrachloride, and finally allowed to dry in air.

Differential Scanning Calorimetry. The PET yarns were cut with the help of scissors into small pieces about 0.5–1 mm long, and 3 mg of the yarn was accurately weighed into an aluminum sample pan. A DuPont Differential Thermal Analyzer Type 990 with the DSC cell was used for recording the thermograms at a heating rate of 10°C/min in a nitrogen gas environment.

X-Ray Diffraction. The crystallinity and crystal sizes were determined from X-ray diffraction measurements, according to the methods described elsewhere.¹¹

Infrared Spectrophotometry. Infrared spectra were recorded on a Perkin-Elmer Infrared Spectrophotometer Model 580B. The powdered samples were dispersed in KBr and pressed into pellets used for these measurements. The 988 cm^{-1} absorption band, which has been identified by Koenig and Hannon¹⁶ to be associated with regular chain folding in PET, was used for characterization of folds.

RESULTS AND DISCUSSION

Glass Transition Temperature

Glass transition temperature (T_g) was taken as the midpoint of the baseline shift region in the DSC thermograms. As shown in Figure 1, T_g shows a systematic variation with heat-setting temperature. For both sets of samples (FA and TA), T_g first increases with heat-setting temperature and then decreases; the maximum T_g is for samples heat-set at 150–160°C. The free-

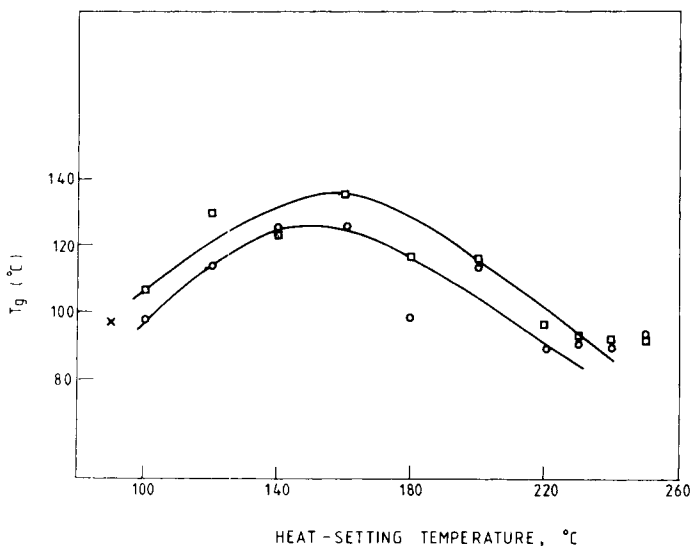


Fig. 1. Variation of T_g with heat-setting temperature: (○) TA; (□) FA; (×) control.

annealed samples, in general, show higher T_g than the corresponding taut-annealed samples.

Crystallinity

Crystallinity was determined using both DSC and X-ray diffraction. In the DSC method, crystallinity was calculated from the area of the melting endotherm, which is a measure of the heat of fusion of the sample (ΔH_{exp}), and the DSC crystallinity, β_{DSC} , is given by

$$\beta_{\text{DSC}} = \Delta H_{\text{exp}} / \Delta H_c$$

where ΔH_c is the heat of fusion of the single crystal. For the purposes of the present calculations, ΔH_c was taken to be 5.8 cal/g, a value given by Wunderlich¹⁷ and used by Fakirov et al.⁶ The X-ray crystallinity was computed using Farrow and Preston's method,¹⁸ which is based on the determination of crystalline and amorphous areas for each sample.

The crystallinity data for the taut-annealed and free-annealed samples are shown in Figures 2 and 3, respectively. It may be emphasized that the DSC crystallinity may not be truly representative of the crystallinity of the samples being investigated, because the samples are subjected to an additional thermal cycle in the DSC and also because the heat of fusion for a perfect crystal is not known with certainty. In further discussion, therefore, the X-ray crystallinity will be taken to represent sample crystallinity.

Crystal Size

The crystal sizes obtained from (010) reflection are shown in Figure 4. There is a considerable increase in crystal size with increasing heat-setting temperature for both FA and TA samples. The free-annealed samples have slightly larger crystals.

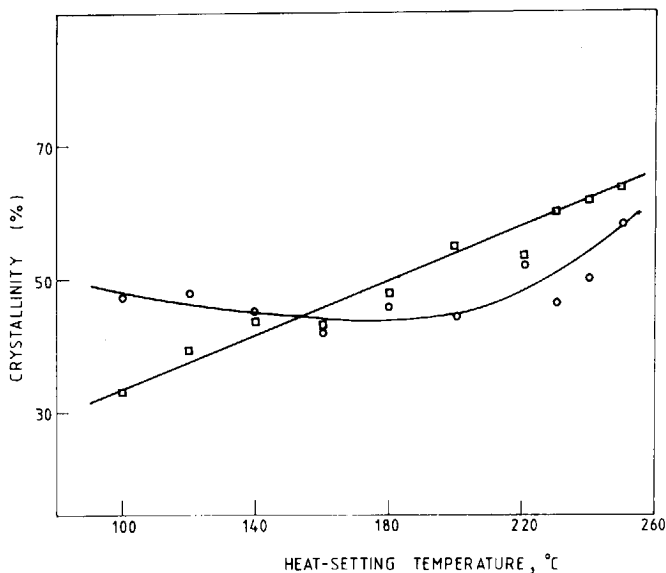


Fig. 2. Variation of crystallinity of TA samples with heat-setting temperature: (○) DSC; (□) X-ray.

Chain Folding

The infrared-spectra for a limited number of samples are shown in Figure 5. It is seen that while the control sample hardly shows any chain folds as measured by the absorption band at 988 cm^{-1} , the free annealed sample heat-set at 240°C shows some chain folding, which in turn appears to be higher than that shown by the TA-250 sample.

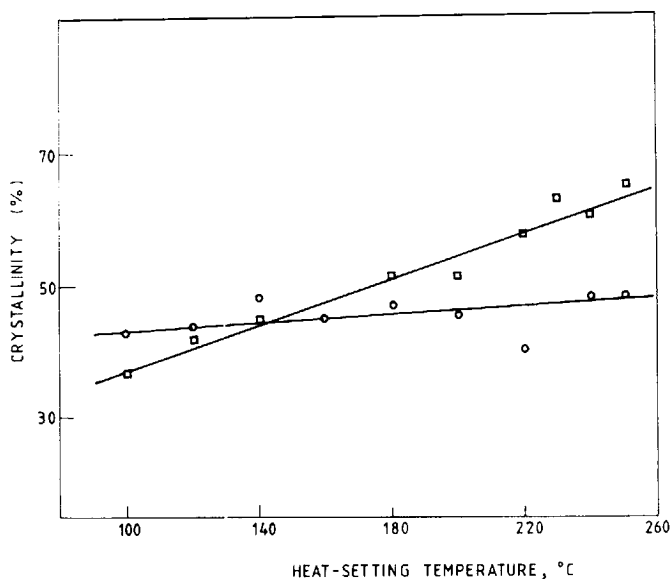


Fig. 3. Variation of crystallinity of FA samples with heat-setting temperature: (○) DSC; (□) X-ray.

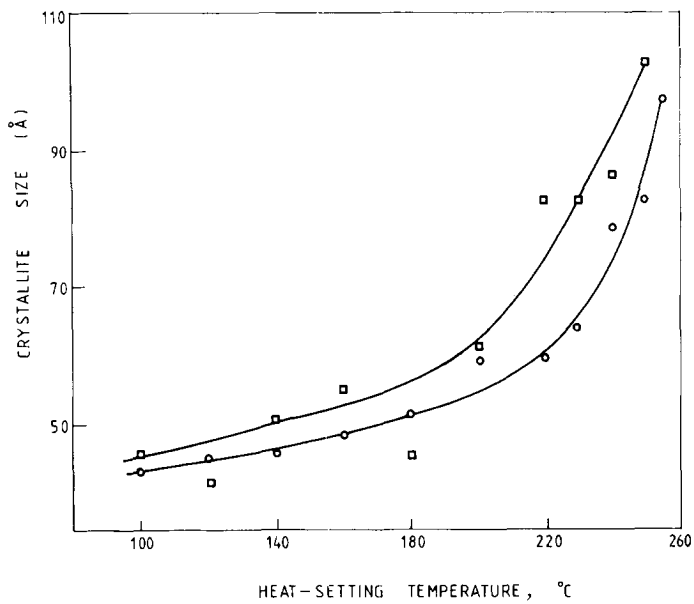


Fig. 4. Crystal size data for TA and FA samples (○) TA; (□) FA.

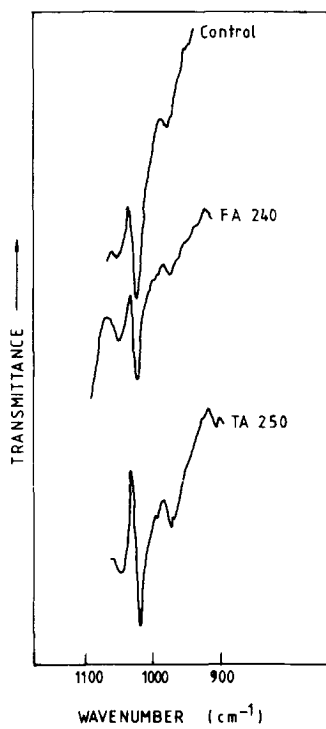


Fig. 5. Chain folding by IR spectrophotometry.

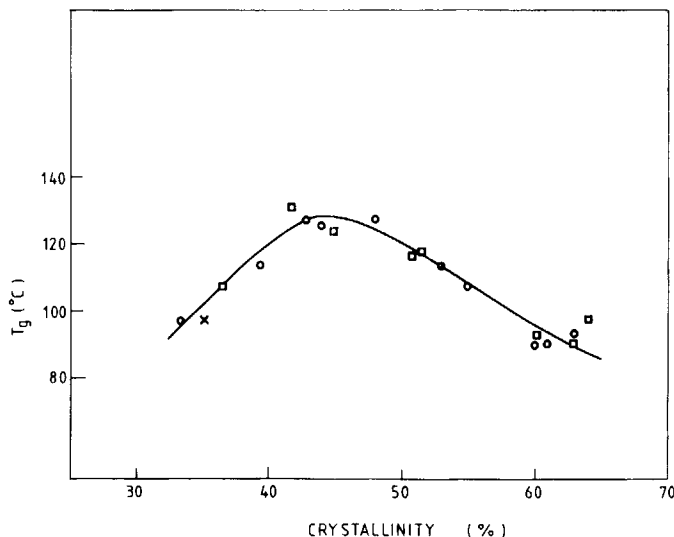


Fig. 6. Dependence of T_g on X-ray crystallinity: (x) control; (o) TA; (□) FA.

Dependence of T_g on Crystallinity

The dependence of T_g on X-ray crystallinity is shown in Figure 6. For both sets of samples, T_g first increases with increasing crystallinity, reaches a peak at about 45% crystallinity, and then decreases. Such an effect has been explored¹⁹ on the basis of size and size distribution of crystallites; high T_g corresponds to a large number of small crystals, which lead to greater constraints on the segmental mobility of the amorphous regions.

Melting Endotherms

Melting endotherms of the TA and FA samples heat-set for 5 min are shown in Figures 7 and 8, respectively; two melting peaks appear at $248 \pm 1^\circ\text{C}$ and $255 \pm 1^\circ\text{C}$ and will be referred to as T_{m1} (endotherm I) and T_{m2} (endotherm II), respectively. Values of T_{m1} and T_{m2} for the various samples are shown in Table I. In keeping with the accepted interpretation, it will be assumed that double melting is observed as long as part of the original structure can reorganize during scanning. Endotherm I corresponds to the melting of crystallites formed at the isothermal crystallization temperature, while endotherm II represents the melting of the less stable fraction which undergoes reorganization. The thermograms show some interesting features, some of which can be discussed in terms of the areas (resolved) of the two endotherms which are measures of the respective heats of fusion, because these areas also represent the noncrystallizable and crystallizable fractions, respectively. The heats of fusion for the first and second endotherms are designated ΔH_1 and ΔH_2 , respectively and are shown in Figures 9 and 10 for taut-annealed and free-annealed samples, respectively. For TA samples, ΔH_1 increases while ΔH_2 decreases with increasing heat-setting temperature; the effects are dramatic at high temperatures. For FA samples, on the other hand, broadly speaking ΔH_1 decreases and ΔH_2 increases.

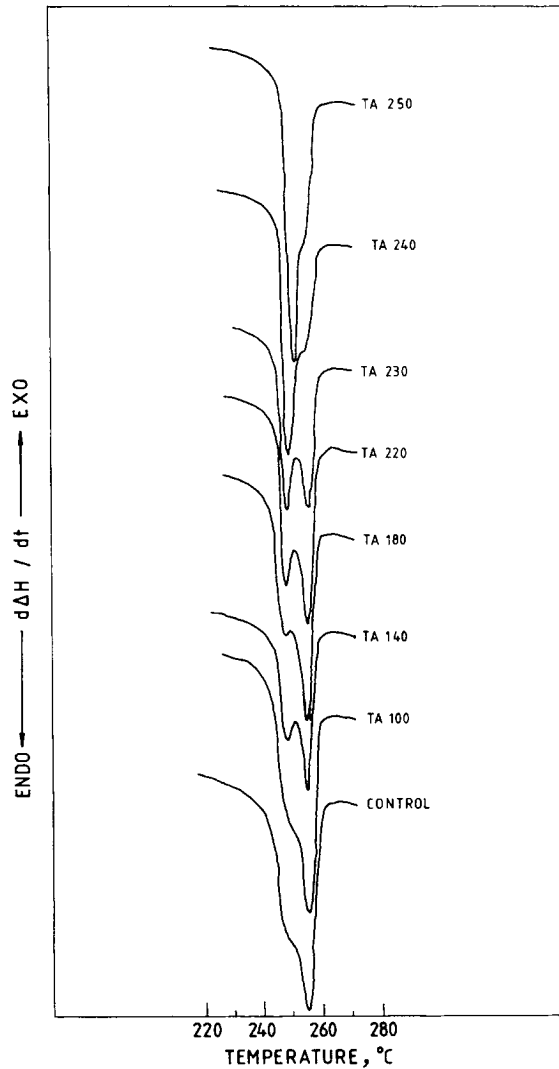


Fig. 7. Melting endotherms of TA samples heat-set for 5 min.

Thus, while in the taut annealed samples the noncrystallizable fraction becomes more predominant as heat-setting temperature increases, in free-annealed samples the crystallizable fraction becomes more predominant. This is indicative of the higher potential for reorganization of the free-annealed samples and will be discussed in greater detail later.

It is observed that in the control sample, endotherm I appears as a shoulder to endotherm II and is thus closer to the endotherms of the free-annealed rather than taut-annealed samples. Previous studies had shown that the structure and mechanical properties of the control sample are very close to those of the taut-annealed samples, particularly those that had been heat-set at the lower temperatures.¹²⁻¹⁵ This observation therefore needs further examination. It may be noted that, during the DSC run, the control

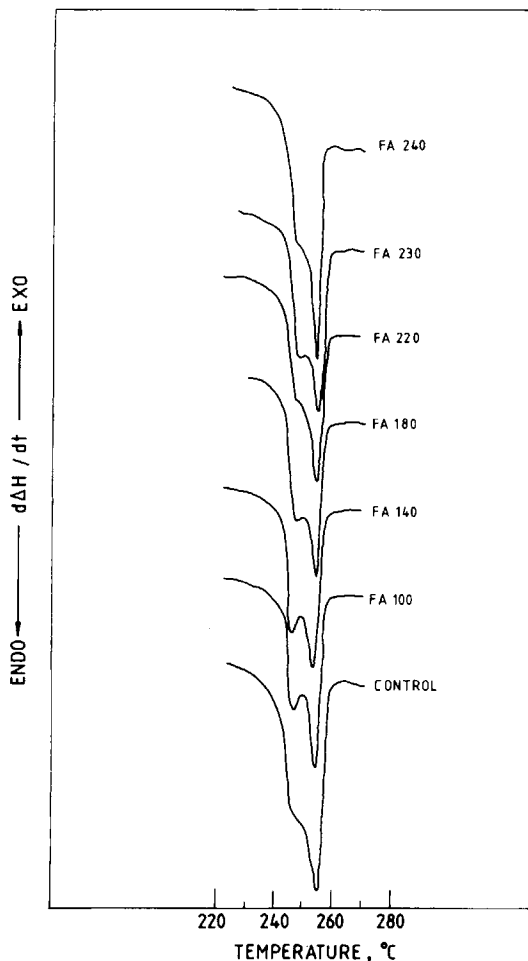


Fig. 8. Melting endotherms of FA samples heat-set for 5 min.

sample is subjected to a thermal cycle for over 20 min over a variable temperature range (20°C to over 250°C) until it gives the first melting peak close to 250°C. During this period the sample is free to shrink; the heat setting is thus close to the free-annealed condition. It is not surprising, therefore, that the control sample shows melting endotherms very similar to the FA-240 sample. This would mean that, as recorded by the present method, the endotherms are not fully representative of the thermal behavior of the control sample. If this point is kept in mind, the data can still be interpreted to yield useful information.

The above argument is indeed relevant to varying degrees for all the melting data, viz., that the effects seen are not entirely those shown by the as-annealed samples but are the combined result of the superposed thermal history during the DSC run on the 5 min isothermal heat-setting history. Nevertheless, a considerable amount of information on the dependence of thermal behavior on structure and morphology can be obtained from these studies as will be clear from what follows. It is noteworthy that the control sample and the TA and FA samples heat-set up to 180°C show similar

TABLE I
Melting Temperatures Corresponding to Two Endotherms of PET Fibers Heat-Set under Different Conditions

Sample	Heat-setting temp (°C)	Heat-setting time (min)	Heat rate (deg/min)	T_{m1} (°C)	T_{m2} (°C)
Control	—	—	10	249	257
TA	100	5	10	247	255
	120	5	10	248	255
	140	5	10	248	255
	160	5	10	247	255
	180	5	10	248	255
	200	5	10	248	255
	220	5	10	245	253
	230	5	10	247	255
	240	5	10	248	255
	250	5	10	249	—
	240	30	10	249	—
	240	60	10	251	—
	250	30	10	250	—
	250	60	10	250	—
	250	60	2	—	—
	250	60	5	—	—
	250	60	20	254	—
250	60	50	257	—	
FA	100	5	10	247	255
	120	5	10	248	256
	140	5	10	246	255
	160	5	10	248	255
	180	5	10	247	255
	200	5	10	247	255
	220	5	10	250	255
	230	5	10	248	255
	240	5	10	248	255
	250	5	10	—	—
	240	30	10	248	254
	240	60	10	250	257
	250	30	10	253	—
	250	60	10	258	—

features; the difference of melting behavior of TA and FA samples is most pronounced for samples heat-set at $240 \pm 10^\circ\text{C}$. This observation also merits some discussion. As has been pointed out, in PET even a less severe thermal treatment when superposed on a more severe treatment can still change the set of PET.^{20,21} The samples heat-set at temperatures close to T_{m1} and T_{m2} (250–258°C) will be expected to show the least effect of superimposed thermal history during the DSC scan and will thus be relatively more representative of the actual effect of heat setting. In the other samples, the thermal effects during scanning, which are superimposed on the heat-setting effects, will predominate.

It was interesting therefore to let the samples which had been heat-set at higher temperatures be set for longer times so that the effect of superimposed thermal history in the DSC is minimized. The data obtained for samples heat-set for longer durations, viz. 30 and 60 min, are shown in

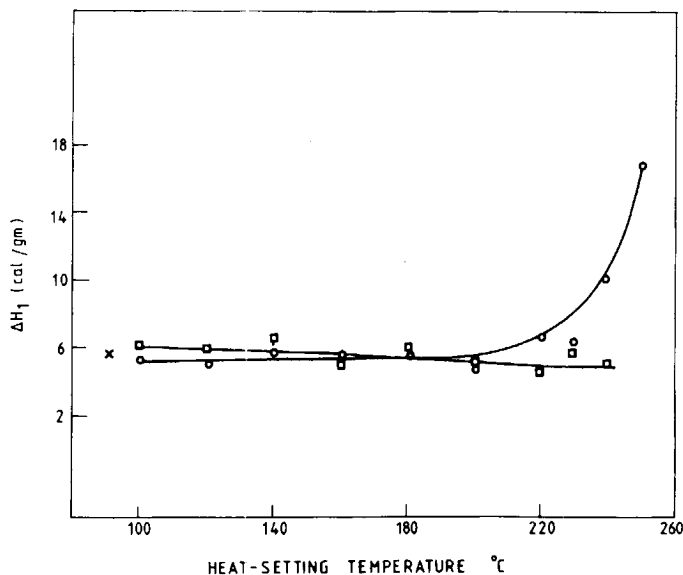


Fig. 9. Heats of fusion of endotherm I: (□) FA; (○) TA; (×) control.

Figure 11 for the sample TA-250 as a typical example. It is seen that at the highest times a single endotherm is obtained. The following interpretation of single endotherm after Groeninckx et al.⁷ will be adopted. They found for isotropic PET crystallized isothermally either a single endotherm for samples crystallized below 150°C or above 215°C; at intermediate crystallization temperatures (150–215°C), two endotherms appeared. Furthermore, according to them, the crystallites obtained at $T_c > 215^\circ\text{C}$ do not transform during scanning and hence give endotherm I. Part of the crys-

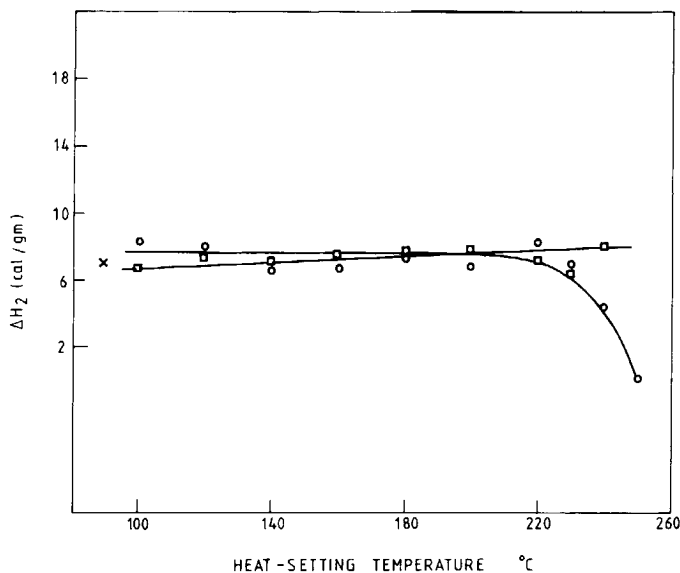


Fig. 10. Heats of fusion of endotherm II: (□) FA; (○) TA; (×) control.

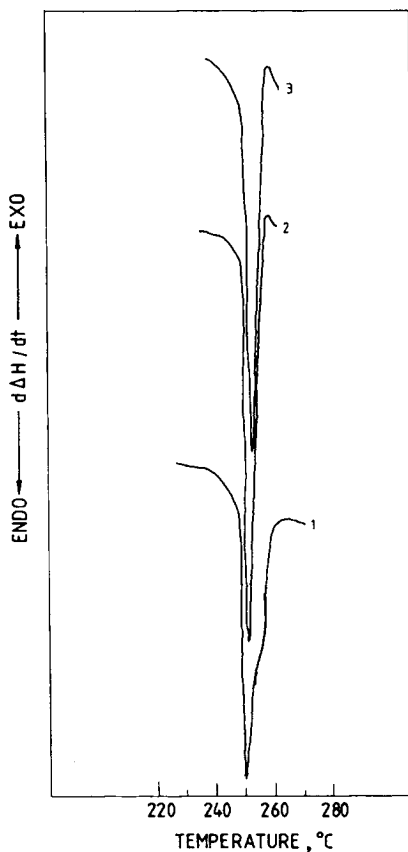


Fig. 11. Melting endotherms for TA-250 sample heat-set for longer times: (1) 5 min; (2) 30 min; (3) 60 min.

tallites formed at lower T_c (150–215°C) can reorganize during heating in the DSC and thus melt at the higher temperature (endotherm II) than the unreorganized fraction (endotherm I); consequently, two endotherms appear. The crystallites formed at $T_c < 150^\circ\text{C}$ completely transform during the DSC run and again one endotherm (endotherm II) is observed. The crystallization of anisotropic fibers is very different from that of the isotropic fibers, but the basic interpretation, we believe, would remain valid though on a different time-temperature scale. In the present case, as is obvious from Figure 11, the samples heat-set at higher temperature for longer times give single endotherms, which are apparently endotherm I. Furthermore, as stated by Sweet and Bell,⁴ this endotherm moves to higher temperature with increase in heating rate; this was verified to be so for these samples.

In the earlier studies it was postulated¹² that with increased time of heat setting, the perfection of crystallites can improve by the disappearance of crystal defects, i.e., dislocations, vacancies, and chain ends can diffuse into the noncrystalline phase. Fakirov et al.⁶ have pointed out that reorganization is rather restrained in PET and crystals can grow at the expense of the neighboring amorphous layers. Groeninckx and co-workers^{8,9} state that

samples heat-set at low temperatures have small, imperfect crystallites, which reorganized by partial melting and recrystallization. In samples heat-set at relatively higher temperatures, no large scale melting occurs; the crystal thickening which occurs without any change in long period has been expected to arise from crystal perfection at the boundary layers of the crystalline and amorphous phases. As observed earlier, the free-annealed samples heat-set at relatively lower temperatures show greater capacity to reorganize during the DSC run compared to the corresponding taut-annealed samples. It is also seen that if the samples are isothermally crystallized at a higher temperature and a longer time, the free-annealed sample has a melting point 8°C higher than the corresponding taut-annealed sample. The free-annealed samples develop larger and more perfect crystals having higher degree of folding. These differences between the taut-annealed and free-annealed samples would be expected to be related to the structural and morphological differences between these two samples. As stated earlier, structurally an important difference is that the amorphous regions in free-annealed samples have much lower orientation and therefore greater molecular mobility. Morphologically, the free-annealed samples have a more well-defined, distinct phase separation of the crystalline and amorphous phases with a predominantly series coupling between the two. It would thus appear that these features allow adjustments to be made in free-annealed samples at the crystal-amorphous boundary layers, which generally occur by diffusion processes, relatively more easily.

Finally, as pointed out by Todoki and Kawaguchi,²² useful information can be obtained by recording thermograms when the fibers are in a constrained state or by using irradiated fibers. This type of study is planned for these samples.

References

1. R. C. Roberts, *J. Polym. Sci. B*, **8**, 381 (1970).
2. M. Ikeda, *Chem. High Polym.*, **25**, (273), 87 (1968).
3. P. A. Holdsworth and A. Turner Jones, *Polymer*, **12**, 195 (1971).
4. G. E. Sweet and J. P. Bell, *J. Polym. Sci., A-2*, **10**, 1273 (1977).
5. A. Miyagi and B. Wunderlich, *J. Polym. Sci., A-2*, **10**, 1401 (1972).
6. S. Fakirov, E. W. Fischer, R. Hoffman, and G. F. Schmidt, *Polymer*, **18**, 1121 (1977).
7. G. Groeninckx, H. Reynaers, H. Berghmans, and G. Smets, *J. Polym. Sci., Polym. Phys. Ed.*, **18**, 1311 (1980).
8. G. Groeninckx and H. Reynaers, *J. Polym. Sci., Polym. Phys. Ed.*, **18**, 1325 (1980).
9. F. Fontaine, J. Ledent, G. Groeninckx, and H. Reynaers, *Polymer*, **23**, 185 (1982).
10. S. W. Shalaby (Chap. 3) and M. Jaffe (Chap. 7), in *Thermal Characterization of Polymeric Materials*, Edith A. Turi, Ed., Academic, New York, 1981.
11. V. B. Gupta and S. Kumar, *J. Appl. Polym. Sci.*, **26**, 1865 (1981).
12. V. B. Gupta and S. Kumar, *J. Polym. Sci., Polym. Phys. Ed.*, **17**, 1307 (1979).
13. V. B. Gupta and S. Kumar, *J. Appl. Polym. Sci.*, **26**, 1885 (1981).
14. V. B. Gupta and S. Kumar, *J. Appl. Polym. Sci.*, **26**, 1877 (1981).
15. V. B. Gupta and S. Kumar, *J. Appl. Polym. Sci.*, **26**, 1897 (1981).
16. J. L. Koenig and M. J. Hannon, *J. Macromol. Sci. Phys.*, **B1**, 119 (1967).
17. B. Wunderlich, *Macromolecular Physics*, Academic, New York, 1973, p. 389.
18. G. Farrow and D. Preston, *Br. J. Appl. Phys.*, **11**, 353 (1960).
19. J. H. Dumbleton and T. Murayama, *Kolloid Z. Z. Polym.*, **220**, 41 (1967).

20. J. G. Cook, *Handbook of Textile Fibres*, 4th ed., Merrow, Watford, U.K., 1968, Vol. II, p. 367.
21. V. B. Gupta and J. Amirtharaj, *Text. Res. J.*, **46**, 785 (1976).
22. M. Todoki and T. Kawaguchi, *J. Polym. Sci., Polym. Phys. Ed.*, **15**, 1507 (1977).

Received December 20, 1983

Accepted April 2, 1984